PAPER

Check for updates

Mechanistic studies on catalytic alkane oxidation by Murahashi's O₂/copper(II)/aldehyde system†

Kohei Yamaguchi, Yuya Uemura, [iD] Hideki Sugimoto, [iD] Rin Ito, Yuma Morimoto [iD] and Shinobu Itoh [iD]*

Mechanistic studies on catalytic alkane hydroxylation by Murahashi's O₂/copper(II)/aldehyde system have been conducted to show that the autoxidation of an aldehyde (RCHO) by an O₂ generating acyl radical intermediate (RC(O)•) is involved as an initiation step of the catalytic cycle. The generated RC(O)• is trapped by O₂ to give an acylperoxyl radical intermediate RC(O)OO•, which may react with another RCHO to generate an adduct intermediate RC(O)OOC(R)(H)O•. The following O–O bond homolytic cleavage of this intermediate will give acyloxyl intermediate RC(O)O• and RCOOH, in which the former acts as a reactive species for hydrogen atom abstraction (HAA) from alkane substrates ($R^1R^2CH_2$; R^1 and R^2 are alkyl groups or hydrogen atoms), giving $R^1R^2CH•$. The generated $R^1R^2CH•$ reacts with O₂ to generate alkylperoxyl radical intermediate $R^1R^2CHOO•$, which then undergoes the Russell reaction to give R^1R^2CHOH (alcohol) and $R^1R^2C=O$ (ketone) in a 1:1 ratio as the oxidation products. The acyloxyl intermediate RC(O)O• also reacts with RCHO to give carboxylic acid RC(O)OH and RC(O)•, constructing the catalytic cycle. The role of copper(II) ions in the above catalytic process is also investigated using a series of copper(II) complexes. Furthermore, Murahashi's system was adopted in the catalytic oxidation of methane.

1. Introduction

Alkanes are abundant chemicals widely found in petroleum and natural gas. Selective C–H bond functionalization of inert alkane substrates is of great importance for converting them into value-added and easily usable organic compounds.[1,2] In particular, selective oxidation of methane, the main component of natural gas and shale gas as well as methane hydrate, into C1 oxygenates such as methanol, formaldehyde and formic acid has been recently attracting much attention in industrial chemistry.[3–8] Therefore, the development of selective oxidation of alkanes including gaseous alkanes has become an important research topic in industrial chemistry as well as in synthetic organic chemistry.[9,10]

Selective oxidation of organic compounds with molecular oxygen (O₂) is one of the most economically and environmentally desirable reactions, since O₂ is abundant and a clean oxidant generating no toxic by-products.[10,11] In this respect, Murahashi's alkane oxidation reaction using O₂ as an oxidant, copper(II) acetate (Cu(OAc)₂) as a catalyst, and acetaldehyde as a sacrificial reductant is an attractive
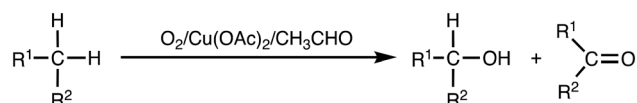
reaction system, where high conversion of alkanes to alcohols and ketones was achieved (Scheme 1).[12–14] Such an O₂/transition-metal/aldehyde catalytic system has also been adopted in the alkene epoxidation reaction, the so-called Mukaiyama epoxidation, where peracids (RC(O)OOH) and/or acyl peroxyl radicals (RC(O)OO•) produced by aldehyde-autoxidation were proposed as reactive oxidants.[15–19] However, mechanistic details of Murahashi's alkane oxidation reaction have yet to be clarified.

In this study, we have conducted detailed mechanistic studies on Murahashi's alkane oxidation reaction to obtain insights into reactive oxidants as well as the catalytic role of metal ions using a series of Cu[II]-complexes. Furthermore, the catalytic system was adopted in the oxidation of methane.

2. Results and discussion

2.1. Catalytic alkane oxidation with the O₂/complex 1/PhCHO system

Murahashi and co-workers reported an efficient alkane oxidation reaction in the presence of acetaldehyde using Cu(OAc)₂ as a catalyst (Scheme 1).[12] In this study, we revisited

Department of Molecular Chemistry, Division of Applied Chemistry, Graduate School of Engineering, Osaka University, 2-1 Yamadaoka, Suita, Osaka 565-0871, Japan. E-mail: shinobu@chem.eng.osaka-u.ac.jp

Scheme 1 Murahashi's alkane oxidation reaction.

This journal is © The Royal Society of Chemistry 2023

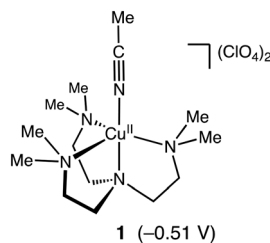*Catal. Sci. Technol.*, 2023, 13, 5859–5867 | 5859

Fig. 1 Structure of complex **1**. Reduction potential of **1** (*vs.* Fc/Fc⁺ in acetonitrile) is shown in parentheses. The cyclic voltammogram of **1** is presented in Fig. S2.†

this reaction system to obtain mechanistic insights into the catalytic alkane oxidation reaction. First, we examined the catalytic oxidation of cyclohexane (CyH) by using [Cu^{II}(Me$_6$-tren)(CH$_3$CN)](ClO$_4$)$_2$ (**1**, Me$_6$tren = tris[2-(dimethylamino) ethyl]amine, see Fig. 1) and benzaldehyde (PhCHO) instead of Cu(OAc)$_2$ and acetaldehyde, respectively. Adoption of the copper(II) complexes enables us to tune the geometry and redox potential of the copper catalyst and the usage of PhCHO allows us to detect the products derived from the aldehyde.

The reaction was started by adding PhCHO (0.2 M) to a CH$_3$CN/CH$_2$Cl$_2$ (v/v = 3/2) mixed solvent solution containing CyH (2.0 M) and a catalytic amount of **1** (0.2 mM) at 40 °C under an O$_2$ atmosphere (Table 1).

Table 1 shows a time-dependent formation of cyclohexanol (**A**), cyclohexanone (**K**), ε-caprolactone (**L**) and chlorocyclohexane (CyCl) monitored by GC-FID. **L** may be generated from **K** *via* the Baeyer–Villiger oxidation by perbenzoic acid, PhC(O)OOH (see below discussion). In this reaction, benzene (PhH) was also obtained. Formation of PhH and CyCl suggests involvement of benzoyloxyl radical (PhC(O)O˙) and cyclohexyl radical (Cy˙) intermediates, respectively (also see below).

To confirm the formation of the cyclohexyl radical (Cy˙) intermediate, the reaction was carried out in a CH$_3$CN/CCl$_4$ mixed solvent (v/v = 3/2) instead of CH$_3$CN/CH$_2$Cl$_2$. As seen

in Table S1,† the formation ratio of CyCl increased from 3% to 17%, clearly demonstrating the formation of Cy˙, since CCl$_4$ has been demonstrated to act as an organic radical trapping agent to give the chlorinated product CyCl.[20]

From the early stage of the catalytic reaction (1 h), **A** and **K** were formed in an almost 1:1 ratio and this ratio was maintained during the reaction as shown in Table 1. If **K** was formed *via* over-oxidation of **A**, **A** should be the main product at the initial stage of the reaction, and the ratio of **K** should increase gradually afterwards. Thus, the results indicate that the reaction involves the "Russell rearrangement" of the tetroxide intermediate (Cy–O–O–O–O–Cy) as shown in Scheme 2.[21] Namely, the cyclohexyl radical intermediate (Cy˙) formed by hydrogen atom abstraction (HAA) from CyH by a reactive oxidant rapidly reacts with O$_2$ at a rate of 10^9 M^{-1} s^{-1} to produce the cyclohexyl–peroxyl radical species (CyOO˙).[22] Radical coupling of two CyOO˙ produces the tetroxide intermediate Cy–O–O–O–O–Cy, from which the Russell rearrangement takes place to give an equal amount of **A** and **K** (Scheme 2). The fact that the amount of **A** slightly exceeded that of **K** in the early stages of the reaction suggests that **A** is also formed directly *via* the reaction of Cy˙ and an oxidant such as perbenzoic acid.

The product distribution pattern was almost the same when the reaction mixture was quenched by PPh$_3$ (Table S2†). Since alkylhydroperoxides (ROOH) are known to be quantitatively converted to the corresponding alcohols (ROH) by the reaction with PPh$_3$,[23] the result indicates that most CyOO˙ was converted to the tetroxide intermediate but not to cyclohexyl hydroperoxide (CyOOH).

To obtain information about the active oxidant, the oxidation reaction of adamantane (AdH) was also examined
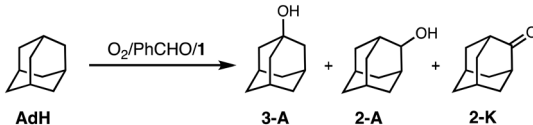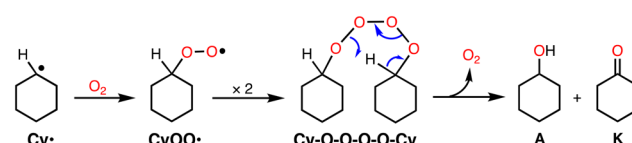
Scheme 2 Russell rearrangement.

Table 1 Oxidation of cyclohexane (CyH) by the O$_2$/**1**/PhCHO system

Time/h	Yield/mM				
	A	**K**	**L**	CyCl	PhH
1	4.0	2.6	0	0.1	0.7
2	9.8	7.8	0.2	0.5	2.3
3	11	9.5	0.4	0.6	2.9
4	15	15	1.2	0.8	3.2
5	17	16	1.2	1.5	5.2

Reaction conditions: [**1**] = 0.2 mM, [PhCHO] = 0.2 M, [cyclohexane] = 2.0 M in CH$_3$CN/CH$_2$Cl$_2$ (v/v = 3/2) at 40 °C under O$_2$. 51 mM benzoic acid (PhCO$_2$H) was obtained after 5 h.

Table 2 Oxidation of adamantane (AdH) by the O_2/**1**/PhCHO system

Substrate	Yield^a/mM			$3°/2°^b$
	3 A	**2-K**	**2-K**	12
Adamantane	16	1.7	2.2	

Reaction conditions: [**1**] = 0.2 mM, [PhCHO] = 0.2 M, [adamantane] = 0.25 M in CH_3CN/CH_2Cl_2 (v/v = 3/2) at 40 °C under O_2. ^{a} The amounts of the products are determined by GC-FID using calibration curves of the products. ^{b} [**3-A**]/([**2-A**] + [**2-K**]) multiplied by 3.

(Table 2). Oxidation of AdH with **1** and PhCHO under O_2 also proceeded efficiently to give the corresponding alcohols (**3-A** and **2-A**) together with a small amount of ketone (**2-K**). It should be noted that the regioselectivity between the secondary and the tertiary carbons was quite high (3°/2° = 12), suggesting that the active intermediate is not a free hydroxy radical (˙OH), since a Fenton-type autoxidation reaction containing ˙OH as a reactive oxidant is known to exhibit almost no regioselectivity (3°/2° ~ 1).[24]
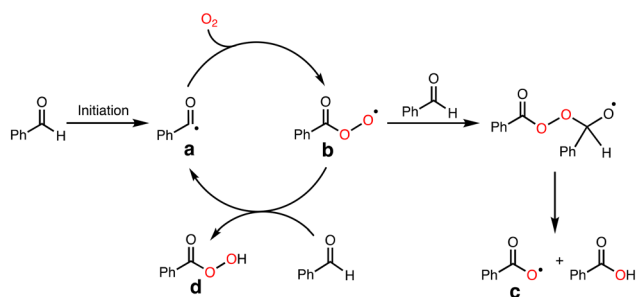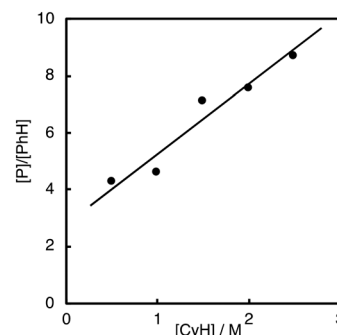
2.2. Reactive oxidants

To explore the reactive oxidants, we focused on the autoxidation of aldehydes. Scheme 3 shows a possible mechanism of the autoxidation of PhCHO.[25–29] First of all, acyl radical intermediate **a** (PhCO˙) is produced by a certain initiating step, which is converted to acyl peroxyl radical intermediate **b** (PhC(O)OO˙) by the reaction with O_2. Then, the generated acyl peroxyl radical intermediate **b** abstracts a hydrogen atom from another molecule of PhCHO, resulting in the formation of peracid **d** (PhC(O)OOH) and **a**, constructing a radical chain cycle. On the other hand, Hutchings and co-workers recently reported that acyloxyl radical intermediate **c** (PhC(O)O˙) is formed through radical adduct formation between **b** and PhCHO and following fragmentation (Scheme 3).[30] Judging from the bond dissociation energy (BDE) of the C–H bond of benzaldehyde (Ph(O)**C–H**, 88.7 ± 2.6 kcal mol^{-1}), the O–H bond of perbenzoic acid (PhC(O)**OO–H**, 96.5 kcal mol^{-1}), and the O–H bond of benzoic acid (PhC(O)**O–H**, 111 ± 4),[31] acyloxy radical
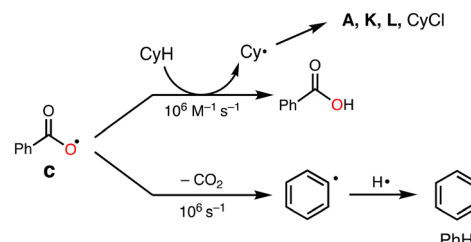
Scheme 4 Competition of HAA with decarboxylation from **c**.

c is the most plausible reactive oxidant for the C–H bond activation of cyclohexane (Cy–**H**, 99.5 kcal mol^{-1}).

It was reported that acyloxy radical **c** is capable of abstracting a hydrogen atom from CyH with a rate constant of about 10^6 M^{-1} s^{-1}.[32] This reaction competes with decarboxylation from **c** with a rate constant of 10^6 s^{-1} to give benzene (PhH) (Scheme 4).[32] Thus, the ratio of the oxidation products (P = **A** + **K** + **L** + CyCl) against benzene (PhH, the decarboxylation product of **c**), [P]/[PhH], is expected to increase as the concentration of the substrate increased, since the hydrogen atom abstraction (HAA) process and decarboxylation reaction are competing.

As clearly seen in Fig. 2, [P]/[PhH] increased as [CyH] is increased. Thus, we concluded that acyloxy radical **c** is a reactive oxidant for the HAA from CyH. The amount of benzoic acid (PhCO$_2$H) formed after 5 h was 51 mM that was larger than the total amount of products (35.7 mM, Table 1). This is reasonable since PhCO$_2$H is formed both *via* the substrate oxidation by PhC(O)O˙ (**c**) (Scheme 4) and *via* the autooxidation of PhCHO (Scheme 3).

Scheme 3 Autoxidation mechanism of benzaldehyde.

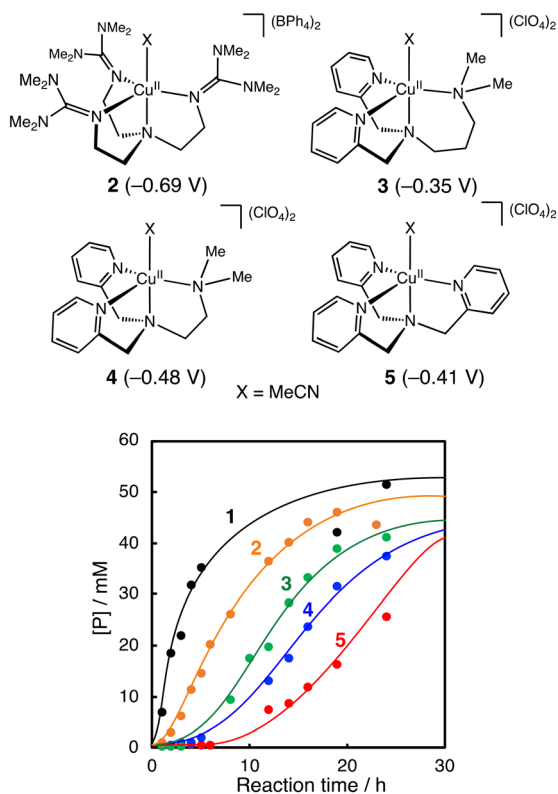**Fig. 2** Dependence of [P]/[PhH] on [CyH].

This journal is © The Royal Society of Chemistry 2023

Catal. Sci. Technol., 2023, **13**, 5859–5867 | **5861**

2 (–0.69 V)   **3 (–0.35 V)**

4 (–0.48 V)   **5 (–0.41 V)**

X = MeCN

Fig. 3 Time courses of product formation in the oxidation of cyclohexane (2.0 M) catalysed by Cu^{II}-complexes (**1–5**, 0.2 mM) with PhCHO (0.2 M) in CH$_3$CN/CH$_2$Cl$_2$ (v/v = 3/2) at 40 °C under O$_2$. [P] = [A] + [K] + [L] + [CyCl]. Reduction potentials of the Cu^{II}-complexes (vs. Fc/Fc$^+$ in acetonitrile) are shown in parentheses. The cyclic voltammograms of the Cu^{II}-complexes are presented in Fig. S2.†

2.3. Catalytic activity of other Cu^{II}-complexes

Fig. 3 compares the catalytic activity of a series of Cu^{II}-complexes **1–5** supported by tripodal tetradentate ligands. Their crystal structures are shown in Fig. S1† together with the crystallographic data in Tables S3–S5.† Among the Cu^{II}-complexes with a similar trigonal bipyramidal structure, complex **1** exhibited the highest initial reaction rate, and the induction period became longer going from **1** to **5**. These results suggest that the Cu^{II}-complexes play an important role in the alkane oxidation reaction.

2.4. Possible role of Cu^{II}-complexes in the initiation step of aldehyde autoxidation

Generation of acyl radical intermediate **a** (Scheme 3) by the reaction of aldehydes and transition-metal complexes has been proposed as the initiation step of aldehyde autoxidation reactions.[33–35] However, little has been examined on the direct reaction between aldehydes and transition-metal complexes.[36,37] To evaluate such a possibility, we tried to trap acyl radical intermediate **a** in CCl$_4$ (Table S6†). Thus, the reaction of complex **1** (2 mM) with an excess amount of PhCHO (0.2 M) was examined in CCl$_4$ under anaerobic conditions (to prevent the reaction of **a** with O$_2$) and then the resulting reaction mixture was poured into methanol. If acyl radical **a**
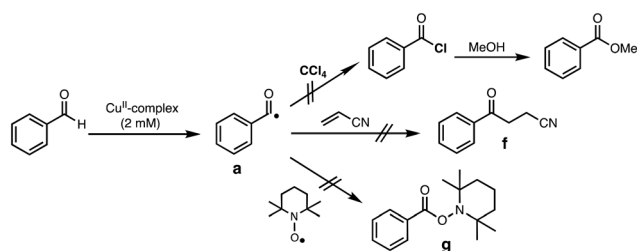
Scheme 5 Acyl radical trapping experiments.

was generated by the reaction of PhCHO and **1**, **a** would be trapped by CCl$_4$ to generate acyl chloride (PhC(O)Cl),[36,38] which will be converted to methyl benzoate (PhC(O)OMe), a more easily detectable product, in methanol (Scheme 5). The same reaction was conducted by using [Cu^{II}(TEPA)OTf](OTf) instead of **1**, since [Cu^{II}(TEPA)OTf](OTf) has a much higher reduction potential (+0.05 V vs. Fc/Fc$^+$) as compared to **1** (–0.51 V). In other words, [Cu^{II}(TEPA)OTf](OTf) is a more powerful oxidant than **1**. In both cases, however, no significant difference was observed in the yield of PhC(O)OMe from that of a blank experiment (without the copper complex).

We also tried to trap **a** using acrylonitrile (Fig. S3†) or TEMPO (Fig. S4†), both of which are known to react with the acyl radical intermediate.[39,40] However, neither the acrylonitrile-adduct **f** nor the TEMPO-adduct **g** were obtained in the presence of complex **1** (Scheme 5).

Furthermore, if the reaction had played a significant role in the initiation step, the length of the induction period in the catalytic oxidation should have a negative correlation with the redox potential of the Cu^{II}-complexes. However, no such correlation was observed (Fig. 3).

All these results strongly suggest that the direct oxidation of benzaldehyde by the Cu^{II}-complex to generate acyl radical intermediate **a** is negligible under the reaction conditions examined in this study.

2.5. Role of Cu^{II}-complexes in peracid activation

In the oxidation of CyH (2.0 M) with PhCHO (0.2 M) and the copper(II) complex under O$_2$, a distinct induction period was
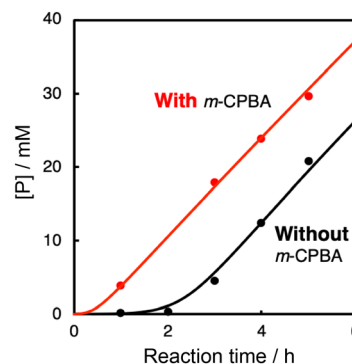

Fig. 4 Time courses of the cyclohexane oxidation by the O$_2$/**1**/PhCHO system with and without m-CPBA (10 mM). Reaction conditions: [**1**] = 0.025 mM, [PhCHO] = 0.2 M, [cyclohexane] = 2.0 M at 40 °C under O$_2$.

5862 | Catal. Sci. Technol., 2023, **13**, 5859–5867

This journal is © The Royal Society of Chemistry 2023

observed in the early stage of the reaction (Fig. 3). Even in the case of complex **1** showing the highest initial rate, the induction period became prominent when the concentration of **1** was reduced from 0.2 mM to 0.025 mM (black line in Fig. 4). On the other hand, addition of 10 eq. (based on **1**) of *m*-CPBA (*m*-chloroperbenzoic acid) at the beginning of the reaction significantly shortened the induction period as shown in Fig. 4 (red line), indicating the important role of peracid **d** generated in the catalytic cycle (see Scheme 3).

We assumed that activation of peracid **d** by the Cu^{II}-complex contributes to the shortening of the induction period. To test this possibility, a direct reaction of **1** and *m*-CPBA was examined spectroscopically (Scheme 6). When 10 eq. of *m*-CPBA was added to an acetonitrile solution of **1** (2 mM), the spectrum changed from black (λ_{max} = 845 nm) to red (λ_{max} = 700 nm) in about 30 min at 40 °C (Fig. 5A), which was different from the spectrum of the *m*-CBA (*m*-chlorobenzoic acid, the decomposition product of *m*-CPBA) adduct of **1** (see Fig. S5†). The generated complex exhibited an ESI-mass spectrum showing a peak cluster, whose peak positions as well as isotope distribution pattern are consistent with the chemical formula of the *m*-CPBA adduct complex of **1** (Fig. S6†). The *m*-CPBA adduct complex was relatively stable at this temperature, but immediately decomposed when 2,4,6-tri-*tert*-butylphenol (10 equiv.) was added to the solution to give a 2,4,6-tri-*tert*-butylphenoxyl radical (the blue spectrum in Fig. 5B).[41] On the other hand, the formation of the phenoxy radical was negligible in the absence of **1**. These results suggest that an adduct formation reaction takes place between the Cu^{II}-complex and peracid **d** generated *in situ* in the catalytic oxidation of CyH by the O_2/Cu^{II}-complex/PhCHO system (Scheme 3).
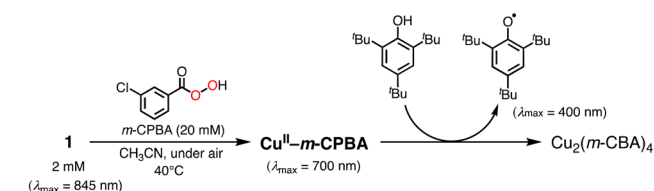
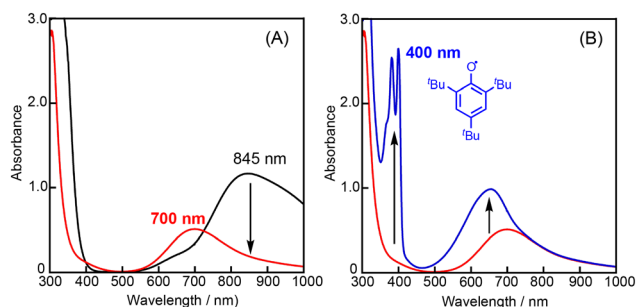**Scheme 6** Reaction of **1** and *m*-CPBA.

Fig. 5 (A) UV-vis spectral change observed upon an addition of *m*-CPBA (10 eq.) to **1** (2 mM) at 40 °C in acetonitrile and (B) UV-vis spectral change of the reaction between the *m*-CPBA adduct Cu^{II}-complex with 2,4,6-tri-*tert*-butylphenol (10 eq.).
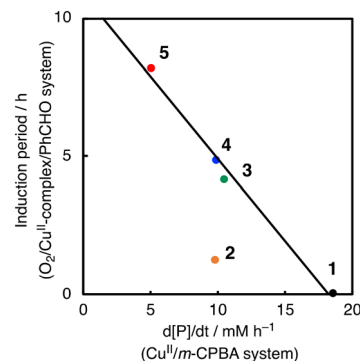

Fig. 6 Correlation between the length of the induction period in the O_2/PhCHO/Cu^{II}-complex system and the catalytic activity of Cu^{II}-complexes in the oxidation of cyclohexane by *m*-CPBA.

To further investigate the role of Cu^{II}-complexes in the peracid activation process, the catalytic oxidation of CyH was performed under anaerobic (N_2) conditions in the presence of **1** and *m*-CPBA. When the catalytic oxidation of CyH (2.0 M) by *m*-CPBA (0.2 M) was carried out in the presence of a catalytic amount of **1** (0.2 mM) in a CH_3CN/CH_2Cl_2 (v/v = 3/2) mixed solvent, **A** was obtained as the major product together with **K**, **L** and **CyCl** as the minor products (Fig. S7†). The catalytic activity of the Cu^{II}-complexes **2**–**5** was also examined under the same conditions (Fig. S7†). Apparently, the Cu^{II}-complexes showed different catalytic activities, which are correlated with the length of the induction period observed in the O_2/Cu^{II}-complex/PhCHO system except **2** as shown in Fig. 6. Namely, the higher the catalytic activity in the *m*-CPBA system, the shorter the induction period in the O_2/Cu^{II}-complex/PhCHO system. Therefore, it can be concluded that the peracid activation by the Cu^{II}-complex accelerates the catalytic reaction of CyH in the early stages of the catalytic reaction. Deviation of complex **2** from the straight line shown in Fig. 6 may be due to steric hindrance of the TMG substituents around the metal center, which prohibits the substrate access to the metal centre. Deactivation of complex **2** by intramolecular hydroxylation of the methyl group of TMG substituents may also cause its lower catalytic activity.[42]

Given the linear correlation shown in Fig. 6 and that the aldehyde autoxidation produces peracids (Scheme 3), the induction phase in the O_2/Cu^{II}-system/PhCHO is thought to involve formation of a Cu^{II}-peracid complex, which cleaves the C–H bond of PhCHO to generate acyl radical intermediate **a**, accelerating the autooxidation reaction of PhCHO (Scheme 3). To obtain mechanistic insights into the peracid activation process in the early stages of the catalytic reaction, we further investigated the induction period phase as below.

As shown in Fig. 7 (black line), there was a prominent induction period of about 2 h, when the lower concentration (0.025 mM) of **1** was used as a catalyst. If the reaction started without adding **1** at the beginning and then **1** was added to the reaction solution after 2 h, there was almost no induction period after the addition of **1** (Fig. 7, blue line). In other words, **1** was not involved in the induction process (first 2 h).
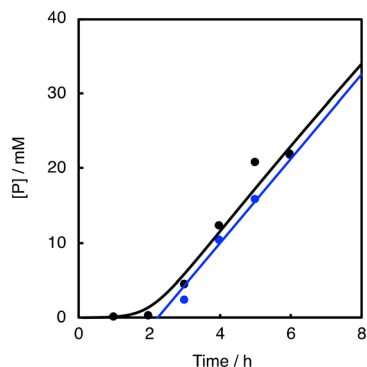
This journal is © The Royal Society of Chemistry 2023

Catal. Sci. Technol., 2023, **13**, 5859–5867 | **5863**

Fig. 7 Time courses of the product formation in the O$_2$/**1**/PhCHO system (black line) and that of the reaction where **1** was added after 2 h (blue line). Reaction conditions: [PhCHO] = 0.2 M, [cyclohexane] = 2.0 M, [**1**]$_0$ = 0.025 mM at 40 °C under O$_2$.

Considering that aldehydes are sensitive to air, the formation of peracids by the oxidation of aldehydes may be the true initiating reaction. Indeed, iodometry revealed that peroxide formation increased with time when PhCHO was stirred in acetonitrile in an O$_2$ atmosphere under conditions that minimized the influence of metal particles, using an aqua regia rinsed vial and stirrer (Fig. S8†). Thus, we concluded that the Cu^{II}-complex played an important role in initiating the aldehyde autoxidation reaction by reacting with the peracid produced by the direct reaction of PhCHO and O$_2$.

2.6. Application to methane oxidation

Finally, oxidation of methane was briefly examined using Murahashi's system. In this reaction, Cu(OAc)$_2$ was used as a catalyst to avoid intramolecular and/or intermolecular ligand hydroxylation (catalyst degradation). Thus, the oxidation of methane was carried out under pressurized conditions (CH$_4$ = 3.0 MPa, O$_2$ = 1.0 MPa) in the presence of Cu(OAc)$_2$ (0.040 µmol) and PhCHO (2.0 mmol) at ambient temperature (25 °C) for 8 h in CH$_3$CN. GC-MS analysis of the final reaction solution indicated the formation of 2.0 µmol methanol as shown in Fig. S9.† Formation of a trace amount of formaldehyde was also noted. The low yield of the oxidation products is apparently due to the higher BDE of methane (105 kcal mol^{-1}) compared to that of CyH (99.5 kcal mol^{-1}) and the lower concentration of the gaseous substrate.

3. Conclusions

In this study, we have conducted a mechanistic study on the catalytic alkane oxidation by an O$_2$/Cu^{II}-complex/RCHO system (Murahashi's reaction). The reaction of RCHO and O$_2$ generates acyl–peroxyl radical RC(O)OO$^•$ intermediate **b** *via* the formation of acyl radical intermediate **a** (Scheme 3). The generated RC(O)OO$^•$ (**b**) abstracts a hydrogen atom from another RCHO to give **a** and peracid **d**, constructing a radical chain cycle. Intermediate **b** also undergoes adduct formation with RCHO to generate the RC(O)OOC(O)(H)O$^•$ intermediate, from which acyloxyl radical **c** and RC(O)OH are produced.

Judging from the high BDE of RC(O)O–H (111 ± 4 kcal mol^{-1}), acyloxyl radical **c** is the most powerful oxidant for the hydrogen atom abstraction (HAA) from the alkane substrate (Scheme 4). Then, the generated alkane radical intermediate undergoes the Russell reaction to give alcohol (**A**) and ketone (**K**) products (Scheme 2).

Regarding the role of the copper(II) complex, we expected that the higher the oxidation ability of the copper(II) complexes, the larger the activation rate of PhCHO, shortening the induction period. However, there was no such correlation between the redox potential of the copper(II) complexes and the length of the induction period (Fig. 3). This is one of the pieces of evidence that the copper(II) complexes do not participate directly to the oxidation of PhCHO to generate acyl radical intermediate **a**. On the other hand, there was a good linear correlation (except complex **2**) between the length of the induction period and the catalytic activity of the copper(II) complexes in the *m*-CPBA system (Fig. 6). This result indicates that the activation of peracid by the copper(II) complex is involved in the induction period of the catalytic oxidation. This assumption is consistent with the result shown in Fig. 7. Thus, we concluded that the significant role of the copper(II) complex is the activation of peracid **d** to generate a copper(II)–peracid adduct intermediate, which may also generate a reactive oxidant to accelerate the autoxidation of RCHO.

Oxidation of methane was briefly examined using Murahashi's system. Judging from the BDEs (RC(O)O–H: 111 ± 4 kcal mol^{-1} *vs.* H$_3$C–H: 105 kcal mol^{-1}), the presumed reactive oxidant, acyloxyl radical **c**, has enough power to induce the HAA from methane. However, the available concentration of methane (3.0 MPa) was too low to compete with the oxidation of PhCHO. Nonetheless, the present study gives important information for the development of efficient catalytic systems for gaseous alkane oxidation reactions.

4. Experimental section

4.1. General

5864 | *Catal. Sci. Technol.*, 2023, **13**, 5859–5867

This journal is © The Royal Society of Chemistry 2023

cryostat cell holder USP-203. Near IR spectra were taken on a Jasco V-670. ^{1}H-NMR spectra were recorded on a JEOL ECP400. Elemental analyses were performed on a Yanaco New Science Inc. CHN order MT-5 or a J-SCIENCE LAB Co., Ltd. MICRO CORDER JM10. ESI-MS (electrospray ionization-mass spectrometry) measurements were performed on a BRUKER cryospray microTOFII. Gas chromatography (flame ionization detector) measurements were performed on a Shimadzu GC-2010 equipped with a GL Science InertCapWAX capillary column (30 m × 0.25 mm), an AOC-20s auto sampler, and an AOC-20i auto injector. Gas chromatography-mass spectrometry (GC-MS) measurements were performed on a Shimadzu GCMS-QP2010 Plus equipped with a RESTEK Rtx-VMS column (30 m × 0.25 mm), an AOC-20s auto sampler, and an AOC-21i auto injector.

4.2. Synthesis

[Cu^{II}(TMG$_3$tren)(CH$_3$CN)](BPh$_4$)$_2$ (2). An acetonitrile solution (1 mL) of Cu^{II}(ClO$_4$)$_2$·6H$_2$O (73 mg, 0.197 mmol) was added to an acetonitrile solution (1 mL) of TMG$_3$tren (87 mg, 0.197 mmol). The colour of the solution changed from pale blue to green. After stirring the mixture for 5 min, the reaction mixture was treated with 2 eq. of NaBPh$_4$ (135 mg, 0.394 mmol). The reaction mixture was added to an excess amount of Et$_2$O to give a pale green precipitate. The resulting solid was collected by filtration and dried under vacuum. Recrystallization from CH$_3$CN/Et$_2$O gave green crystals suitable for X-ray crystallographic analysis: 43 mg, 18%. ESI-MS (pos): m/z = 538.31, calcd. for ([Cu^{II}(TMG$_3$tren)Cl]$^+$) 538.30. Elemental anal: calcd. for ([Cu^{II}(TMG$_3$tren)(CH$_3$CN)(BPh$_4$)$_2$]) (CuC$_{71}$H$_{91}$N$_{11}$B$_2$): C; 71.80, H; 8.06, N; 12.97. Found: C; 71.79, H; 7.96, N; 13.08.

[Cu^{II}(Me$_2$-pp3)(CH$_3$CN)](ClO$_4$)$_2$ (3). An acetonitrile solution (2.0 mL) of Cu^{II}(ClO$_4$)$_2$·6H$_2$O (324 mg, 0.875 mmol) was added to an acetonitrile solution (1.5 mL) of Me$_2$-pp3 (249 mg, 0.875 mmol). The colour of the solution changed from pale blue to deep blue. After stirring for 5 min, the reaction mixture was added to an excess amount of Et$_2$O to give a blue precipitate. The resulting solid was collected by filtration and dried under vacuum. Recrystallization from CH$_3$CN/Et$_2$O gave blue crystals: 86 mg, 17%. ESI-MS (pos): m/z = 382.10, calcd. for ([Cu^{II}(Me$_2$-pp3)Cl]$^+$) 382.10. Elemental anal: calcd. for ([Cu^{II}(Me$_2$-pp3)(CH$_3$CN)(ClO$_4$)$_2$]) (CuC$_{19}$H$_{27}$N$_5$Cl$_2$O$_8$): C; 38.82, H; 4.63, N; 11.91. Found: C; 38.78, H; 4.70, N; 11.95.

[Cu^{II}(Me$_2$-uns-penp)(CH$_3$CN)](ClO$_4$)$_2$ (4). This compound was prepared by a similar procedure to that for the synthesis of [Cu^{II}(Me$_2$-pp3)(CH$_3$CN)](ClO$_4$)$_2$ (3): 41 mg, 20%. ESI-MS (pos): m/z = 368.08, calcd. for ([Cu^{II}(Me2-uns-penp)Cl]$^+$) 368.08. Elemental anal: calcd. for ([Cu^{II}(Me$_2$-uns-penp)(CH$_3$CN)(ClO$_4$)$_2$]) (CuC$_{18}$H$_{25}$N$_5$Cl$_2$O$_8$): C; 37.80, H; 4.37, N; 12.20. Found: C; 37.16, H; 4.31, N; 12.12.

4.3. X-ray crystallographic analysis

Single crystals of the copper(II) complexes were mounted on a DT-MicroLoop (MiTegan, LLC) with mineral oil. X-ray diffraction data were collected on a Rigaku R-AXIS RAPID diffractometer using filtered MoKα radiation (λ = 0.71075 Å). Direct methods with SHELXT were used for the structure solution of the crystals. All calculations were performed with the observed reflections $[I > 2\sigma(I)]$ with the Olex2 crystallographic software packages except for refinement which was performed using SHELXL. Hydrogen atoms were refined using a riding model. CCDC 2262940–2262944 contain the supplementary crystallographic data (CIF files) for the copper(II) complexes (**1–5**).

4.4. Catalytic oxidation of the O$_2$/Cu(II)-complex/aldehyde system

All procedures of the catalytic oxidation reactions were carried out under an O$_2$ atmosphere using an O$_2$ balloon unless otherwise noted. The reaction was started by adding an aldehyde to a mixed solvent (CH$_3$CN/CH$_2$Cl$_2$, v/v = 3/2) containing a copper(II) complex and a substrate. After quenching the reaction by passing the reaction mixture through an alumina-column, products were analysed by GC-FID. All peaks of interest were identified by comparing the retention times with those of the authentic samples. The products were quantified by comparing their peak areas with that of an internal standard (nitrobenzene) using calibration curves consisting of plots of molar ratio (moles of organic compound/moles of internal standard) *versus* area ratio (area of organic compound/area of standard).

4.5. Catalytic oxidation of the *m*-CPBA/Cu(II) system

The reaction was started by adding *m*-CPBA to a mixed solvent (CH$_3$CN/CH$_2$Cl$_2$, v/v = 3/2) containing a copper(II) complex and a substrate under N$_2$. After quenching the reaction by passing the reaction mixture through an alumina-column, products were analysed by GC-FID. All peaks of interest were identified by comparing the retention times with those of the authentic samples. The products were quantified by comparing their peak areas with that of an internal standard (nitrobenzene) using calibration curves consisting of plots of molar ratio (moles of organic compound/moles of internal standard) *versus* area ratio (area of organic compound/area of standard).

4.6. Acyl radical trapping experiment by CCl$_4$

PhCHO (100 eq.) was added to an CH$_3$CN/CCl$_4$ (v/v = 3/2) solution (2.5 mL) of a copper(II)-complex (0.2 mM). The reaction mixture was stirred for 9 days at room temperature under N$_2$. After quenching the reaction by adding 1 mL of CH$_3$OH into the reaction mixture, products were analysed by GC–MS and GC-FID.

4.7. Oxidation of methane

The oxidation of methane was conducted under pressurized conditions using a methane/oxygen gas mixture in a high-pressure reactor. After quenching the reaction using a silica column, the products were analysed by using GC-MS. All

This journal is © The Royal Society of Chemistry 2023

Catal. Sci. Technol., 2023, **13**, 5859–5867 | **5865**

peaks of interest were identified by comparing the retention times and mass spectra with those of the authentic samples. The products were quantified by comparing their peak areas with that of an internal standard (nitrobenzene) using a calibration curve consisting of a plot of mole ratio (moles of organic compound/moles of internal standard) *versus* area ratio (area of organic compound/area of internal standard).

Author contributions

S. I. conceived the idea and designed the project. K. Y. and Y. U. performed most of the experiments. H. S. contributed to X-ray crystallographic analysis. Y. M. was involved in the discussion of the reaction mechanism. S. I. and K. Y. wrote the manuscript. All the authors commented on the final draft of the manuscript and contributed to the analysis and interpretation of the data.

Conflicts of interest

There are no conflicts to declare.

Acknowledgements

Notes and references

1 A. E. Shilov and G. B. Shul'pin, *Chem. Rev.*, 1997, **97**, 2879–2932.

2 V. K. Ahluwalia, *Oxidation in organic synthesis*, CRC Press, Boca Raton, 2012.

3 R. H. Crabtree, *Chem. Rev.*, 1995, **95**, 987–1007.

4 N. J. Gunsalus, A. Koppaka, S. H. Park, S. M. Bischof, B. G. Hashiguchi and R. A. Periana, *Chem. Rev.*, 2017, **117**, 8521–8573.

5 P. Schwach, X. Pan and X. Bao, *Chem. Rev.*, 2017, **117**, 8497–8520.

6 V. C. C. Wang, S. Maji, P. P. Y. Chen, H. K. Lee, S. S. F. Yu and S. I. Chan, *Chem. Rev.*, 2017, **117**, 8574–8621.

7 B. E. R. Snyder, M. L. Bols, R. A. Schoonheydt, B. F. Sels and E. I. Solomon, *Chem. Rev.*, 2018, **118**, 2718–2768.

8 Y. Tang, Y. Li and F. Tao, *Chem. Soc. Rev.*, 2022, **51**, 376–423.

9 C.-M. Che, V. K.-Y. Lo, C.-Y. Zhou and J.-S. Huang, *Chem. Soc. Rev.*, 2011, **40**, 1950–1975.

10 C. Tang, X. Qiu, Z. Cheng and N. Jiao, *Chem. Soc. Rev.*, 2021, **50**, 8067–8101.

11 T. Punniyamurthy, S. Velusamy and J. Iqbal, *Chem. Rev.*, 2005, **105**, 2329–2364.

12 S.-I. Murahashi, Y. Oda, T. Naota and N. Komiya, *J. Chem. Soc., Chem. Commun.*, 1993, 139–140.

13 Y. Hayashi, N. Komiya, K. Suzuki and S.-I. Murahashi, *Tetrahedron Lett.*, 2013, **54**, 2706–2709.

14 H. Sterckx, B. Morel and B. U. W. Maes, *Angew. Chem., Int. Ed.*, 2019, **58**, 7946–7970.

15 K. R. Lassila, F. J. Waller, S. E. Werkheiser and A. L. Wressell, *Tetrahedron Lett.*, 1994, **35**, 8077–8080.

16 N. Mizuno, H. Weiner and R. G. Finke, *J. Mol. Catal. A: Chem.*, 1996, **114**, 15–28.

17 W. Nam, H. J. Kim, S. H. Kim, R. Y. N. Ho and J. S. Valentine, *Inorg. Chem.*, 1996, **35**, 1045–1049.

18 B. B. Wentzel, P. A. Gosling, M. C. Feiters and R. J. M. Nolte, *J. Chem. Soc., Dalton Trans.*, 1998, 2241-2246, DOI: 10.1039/A801175C.

19 B. B. Wentzel, P. L. Alsters, M. C. Feiters and R. J. M. Nolte, *J. Org. Chem.*, 2004, **69**, 3453–3464.

20 T. Shinke, M. Itoh, T. Wada, Y. Morimoto, S. Yanagisawa, H. Sugimoto, M. Kubo and S. Itoh, *Chem. – Eur. J.*, 2021, **27**, 14730–14737.

21 G. A. Russell, *J. Am. Chem. Soc.*, 1957, **79**, 3871–3877.

22 B. Maillard, K. U. Ingold and J. C. Scaiano, *J. Am. Chem. Soc.*, 1983, **105**, 5095–5099.

23 I. Garcia-Bosch and M. A. Siegler, *Angew. Chem., Int. Ed.*, 2016, **55**, 12873–12876.

24 L. Cermenati, D. Dondi, M. Fagnoni and A. Albini, *Tetrahedron*, 2003, **59**, 6409–6414.

25 H. R. Cooper and H. W. Melville, *J. Chem. Soc.*, 1951, 1984–1993.

26 H. R. Cooper and H. W. Melville, *J. Chem. Soc.*, 1951, 1994–2002.

27 W. A. Waters and C. Wickham-Jones, *J. Chem. Soc.*, 1951, 812–823.

28 J. R. McNesby and T. W. Davis, *J. Am. Chem. Soc.*, 1954, **76**, 2148–2152.

29 G. E. Zaikov, J. A. Howard and K. U. Ingold, *Can. J. Chem.*, 1969, **47**, 3017–3029.

30 M. Sankar, E. Nowicka, E. Carter, D. M. Murphy, D. W. Knight, D. Bethell and G. J. Hutchings, *Nat. Commun.*, 2014, **5**, 3332.

31 Y.-R. Luo, *Conprehensive Handbook of Chemical Bond Energy*, CRC Press, Boca Raton, London, New York, 2007.

32 J. Chateauneuf, J. Lusztyk and K. U. Ingold, *J. Am. Chem. Soc.*, 1988, **110**, 2877–2885.

33 C. E. H. Bawn and J. B. Williamson, *Trans. Faraday Soc.*, 1951, **47**, 721–734.

34 C. E. H. Bawn and J. E. Jolley, *Proc. R. Soc. London, Ser. A*, 1956, **237**, 297–312.

35 C. H. E. Bawn, T. P. Hobin and L. Raphael, *Proc. R. Soc. London, Ser. A*, 1956, **237**, 313–324.

36 C. Chatgilialoglu, D. Crich, M. Komatsu and I. Ryu, *Chem. Rev.*, 1999, **99**, 1991–2070.

37 I. V. Alabugin, L. Kuhn, M. G. Medvedev, N. V. Krivoshchapov, V. A. Vil', I. A. Yaremenko, P. Mehaffy, M. Yarie, A. O. Terent'ev and M. A. Zolfigol, *Chem. Soc. Rev.*, 2021, **50**, 10253–10345.

38 S. Winstein and F. H. Seubold Jr., *J. Am. Chem. Soc.*, 1947, **69**, 2916–2917.

39 G.-Z. Wang, R. Shang, W.-M. Cheng and Y. Fu, *Org. Lett.*, 2015, **17**, 4830–4833.

40 W. Liu, Y. Li, K. Liu and Z. Li, *J. Am. Chem. Soc.*, 2011, **133**, 10756–10759.

41 V. W. Manner, T. F. Markle, J. H. Freudenthal, J. P. Roth and J. M. Mayer, *Chem. Commun.*, 2008, 256–258.

5866 | *Catal. Sci. Technol.*, 2023, **13**, 5859–5867

This journal is © The Royal Society of Chemistry 2023

42 F. F. Pfaff, F. Heims, S. Kundu, S. Mebs and K. Ray, *Chem. Commun.*, 2012, **48**, 3730–3732.

43 D. D. Perrin, W. L. F. Armarego and D. R. Perrin, *Purification of Laboratory Chemicals*, Pergamon Press, Elmsford, NY, 4th edn, 1996.

44 J. W. Canary, Y. Wang, R. Roy Jr. , J. L. Que and H. Miyake, in *Inorganic Syntheses*, 1998, pp. 70–75, DOI: 10.1002/9780470132630.ch11.

45 K. D. Karlin, J. C. Hayes, J. P. Hutchinson, J. R. Hyde and J. Zubieta, *Inorg. Chim. Acta*, 1982, **64**, L219–L220.

46 T. Brückmann, J. Becker, C. Würtele, M. T. Seuffert, D. Heuler, K. Müller-Buschbaum, M. Weiß and S. Schindler, *J. Inorg. Biochem.*, 2021, **223**, 111544.

47 H. Wittmann, V. Raab, A. Schorm, J. Plackmeyer and J. Sundermeyer, *Eur. J. Inorg. Chem.*, 2001, **2001**, 1937–1948.

48 F. Mehlich, A. E. Roberts, M. Kerscher, P. Comba, G. A. Lawrance, C. Würtele, J. Becker and S. Schindler, *Inorg. Chim. Acta*, 2019, **486**, 742–749.

49 Y. J. Choi, K.-B. Cho, M. Kubo, T. Ogura, K. D. Karlin, J. Cho and W. Nam, *Dalton Trans.*, 2011, **40**, 2234–2241.

50 J. Wang, M. P. Schopfer, S. C. Puiu, A. A. N. Sarjeant and K. D. Karlin, *Inorg. Chem.*, 2010, **49**, 1404–1419.

51 V. V. Smirnov and J. P. Roth, *J. Am. Chem. Soc.*, 2006, **128**, 3683–3695.